ACS OMEGA

http://pubs.acs.org/journal/acsodf

Article

Hybrid Device of Blue GaN Light-Emitting Diodes and Organic Light-Emitting Diodes with Color Tunability for Smart Lighting Sources

Yalian Weng, Guixiong Chen, Junyang Nie, Sihua Que, Suk-Ho Song, Yongshen Yu, Fan Zhang, Hengshan Liu, Xiongtu Zhou,* Yongai Zhang,* Jie Sun, Jang-Kun Song, Chaoxing Wu, Tailiang Guo, and Qun Yan*

Cite This: *ACS Omega* 2022, 7, 5502−5509

Read Online

ACCESS | Metrics & More | Article Recommendations

ABSTRACT: A lighting device with a wide color-tunable range is still a challenge for lighting based on either organic light-emitting diodes (OLEDs) or inorganic LEDs. In this work, we first proposed a novel hybrid device of organic LEDs and inorganic blue GaN LEDs to achieve full white and other colors. Organic LEDs were stacked with green and red emissive layers and connected with blue GaN LEDs in parallel but in opposite polarity voltage. Under the alternate-current (AC) driving, the hybrid structure can be controlled independently by applying timing variable opposite voltages to emit the light from either blue LEDs or the stacked OLEDs for forming mixed colors. The hybrid device can generate white light, varying in a wide range by changing the amplitude and duty ratio (DR) of AC-driving signals, from cold white to standard white and to warm white (3668−11 833 K). When an AC voltage of (4.80 V, −2.45 V) was applied, the device has a high color gamut of 95.24% National Television System Committee (NTSC) and a high color rendering index (R_a) of 92.4%. The novel hybrid device with the blue LED and OLED in opposite polarity exhibits potential applications in smart solid-state lighting, display, and light communication.

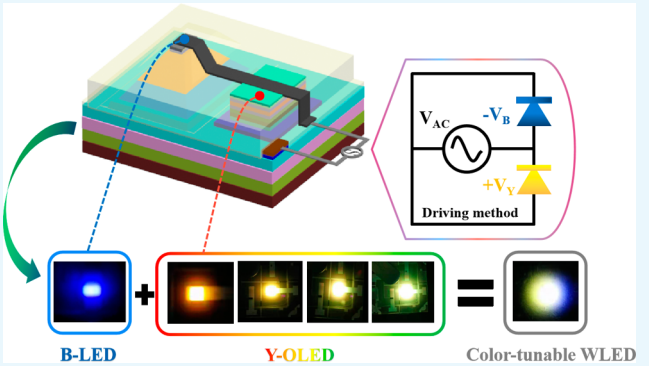

1. INTRODUCTION

In comparison to traditional light sources such as incandescent lamps and fluorescent lamps, white light-emitting diodes (WLEDs) possess great competitive advantages of environmental friendliness, high response speed, high efficiency, low power consumption, and longevity and have been widely used in lighting fields of indoor lighting, headlights, street lamps, and backlight.[1−5] The most common way to fabricate WLEDs is to combine blue inorganic LEDs or organic LEDs with broad color fluorescent materials or to create individually addressable light with excitation wavelengths of red (R), green (G), and blue (B).[6−9] As for inorganic WLEDs, it is difficult to grow the multiple quantum wells (MQWs) of three RGB colors on the same epitaxial wafer, and the method requires a precise alignment for each pixel and complicated driving circuit to maintain the color rendering index (CRI) during operation.[10−12] Also, the low efficiency of green GaN LEDs prohibited using RGB LEDs for highly efficient lighting applications. Therefore, the integration of yellow phosphor with high-intensity GaN blue LEDs was widely adopted. The color conversion layers are converted to emit yellow light after absorbing the blue LED light and the mix of blue light from the LED and yellow light from phosphor to form white light. $Y_3Al_5O_{12}:Ce^{3+}$ (YAG) yellow phosphor was used at the early stage, but such WLEDs suffered from low CRI (R_a < 80), high correlated color temperature (CCT, ∼6500 K), and low color gamut due to the absence of the red component.[13−16] The CRI can be improved by adding red phosphor at the cost of lowering the luminous efficacy. The neutral and highly efficient warm color lighting from inorganic WLEDs is still unsatisfactory and needs to be further developed. For color-tunable organic light-emitting diode (OLED) lighting, the stack of a red OLED, green OLED, and blue OLED or strip type of RGB OLED is the way to make color-tunable and high-CRI lighting devices, but the low energy efficiency and poor lifetime of blue OLEDs make color-tunable OLED lighting devices have poor energy efficiency and product longevity. Cost remains the number one challenge for the OLED light industry; ink-jet printing or roll-to-roll manufacturing might be able to reduce

Received: December 8, 2021
Accepted: January 19, 2022
Published: January 31, 2022

© 2022 The Authors. Published by American Chemical Society

the manufacturing cost. Ink-jet printing is usually employed to prepare RGB pixels in pre-made banks, which allows precise patterning of the emissive layer (EML) with a negligible material waste but has some shortcomings such as high requirement for solvents and film-forming conditions, poor uniformity (e.g., coffee ring), and low luminous efficacy and is far from mass production.[17−19] To overcome these issues, full-color-tunable OLEDs by vertically stacking R, G, and B-OLEDs using evaporation have been proposed, whose intensity and color can by controlled by the voltage applied.[20−22] However, it also requires complex circuit design and fabrication, including four independently addressable electrodes to drive these devices. The tandem WOLEDs have much higher voltage, higher power consumption, and lower power efficiency than those of single-unit WOLEDs.[22] Moreover, the color adjustment of these white light devices can only be in a small range of intensity or CCT.[23,24] However in daily life, a larger range of color-tunable lighting is required, such as choosing the white light with different CCTs in different weathers or different environments, so as to get better visual lighting effects.

Aiming at the above problems, a large number of researchers have made great efforts to improve the performance of WLEDs.[25−28] In recent years, quantum dots (QDs) with unique properties of narrow emission spectra, tunable wavelength, and high quantum efficiency (QY) have been widely used as the color converting materials, resulting in high CRI and high color gamut.[29−34] Professor Kuo's team has applied CdTe QDs to blue LEDs and obtained more than 92% R_a and 90% NTSC.[35] Furthermore, professor Chen's team has developed a multifunctional color-tunable device by a hybrid structure of tandem QLED and OLED devices, which was realized by stacking a yellow CdSe QDs (Y-QLED) with a blue OLED (B-OLED) using an IZO intermediate connecting electrode.[36] The device could achieve white light illumination and full color display under DC and alternate-current (AC) driving, although the CRI and color gamut were only 60 and 63% NTSC, respectively. However, the semiconductor materials of CdSe and CdTe QDs with high QY tend to be toxic, limiting their commercial application, while non-toxic InP QDs suffer from low efficiency. QDs are extremely sensitive to oxygen (O_2) moisture vapor (H_2O) and heat.[37−39] On the other hand, the stability and lifetime of blue OLEDs are far from commercial standards, and there is still a long way to go.[40−42]

As part of our innovation of hybrid structure of the GaN LED and organic LED,[43] a novel color-tunable hybrid LED device was first demonstrated, which was realized by connecting a yellow organic LED (YOLED) with a blue inorganic LED (BLED) in parallel but in opposite polarity. The YOLED was stacked by a green EML with a red EML using a hole delay layer (HDL) in series, whose purity can be controlled by the magnitude of voltage and the thickness of HDL. With such a configuration, the hybrid LED worked under AC driving, and the intensity of R, G, and B primary colors was easily adjustable through the variation of AC driving voltage and duration of time, leading to the difference of CCT (3668−11 833 K), changing from cold white to warm white, and exhibited a high CRI of 92.4% (R_a).

2. RESULTS AND DISCUSSION

2.1. Design of the Hybrid LED Device. Color-tunable devices with a two-terminal simple circuit are the goals that have long been pursued. The designed structure of the hybrid LED device, as shown in Figure 1, is composed of a BLED and

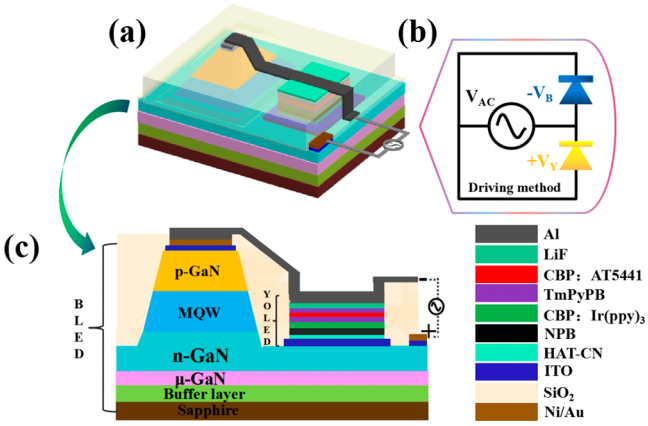

Figure 1. Device structure and driving method of the hybrid LED device. (a) Schematic illustration of the designed structure and the (b) drive method. (c) Cross-section view of the hybrid LED.

YOLED, which are arranged in parallel with each other in the horizontal direction. The p pad of the BLED and the cathode of the YOLED are connected as the negative electrode of the hybrid LED, and the n pad of the BLED is connected with the anode of the YOLED to be the positive electrode of the hybrid LED. In this way, the YOLED is forwardly driven, while the BLED is reversely biased, and thus, both devices can be independently addressed by the polarity of the driving voltage. The hybrid device emits yellow light at a positive voltage and blue light at a negative voltage, and the two simultaneously glow and mix to form white light under voltage pulse train with various magnitudes and duration.

Improving the charge balance of the device has always been a concern and extensively studied issue. OLED is the hole excess device, and the mobility of holes is much greater than that of electrons.[44,45] Conventionally, without TmPyPB sandwiched between the red EML and the green EML, holes accumulate at the ETL interface, resulting in an unbalanced carrier, which greatly reduces the luminous efficiency of the device. In this work, a HDL of TmPyPB was adopted, which is a key strategy for the realization of color change and the promotion of YOLED's performance. With different thicknesses of the HDL, the holes transporting will be delayed into the red EML, to a certain extent, and the mobility of carriers is different at high and low voltages, resulting in the migration of the recombination region and thus emitting different yellow light. Therefore, by varying the thicknesses of HDL and the magnitude of the applied voltage, the ratio of red and green light can be controlled to obtain different colors of yellow light of the device, which will be discussed later.

2.2. Fabrication and Optimization of YOLEDs. The color and performance of YOLEDs are closely related to the thickness of the HDL. In order to get excellent YOLEDs, several OLED samples with different HDL thicknesses were fabricated on the patterned indium−tin−oxide (ITO), and the electrical characteristics were investigated and are shown in Figure 2. The HDL thickness varied from 0, 1, 2, 3, 4 to 5 nm. As described in the electroluminescence (EL) spectra in Figure 2a, without the HDL, hole mobility was much greater than electron mobility at low voltage, and the carriers met and combined in the red EML, emitting red light only. With the

https://doi.org/10.1021/acsomega.1c06934
ACS Omega 2022, 7, 5502−5509

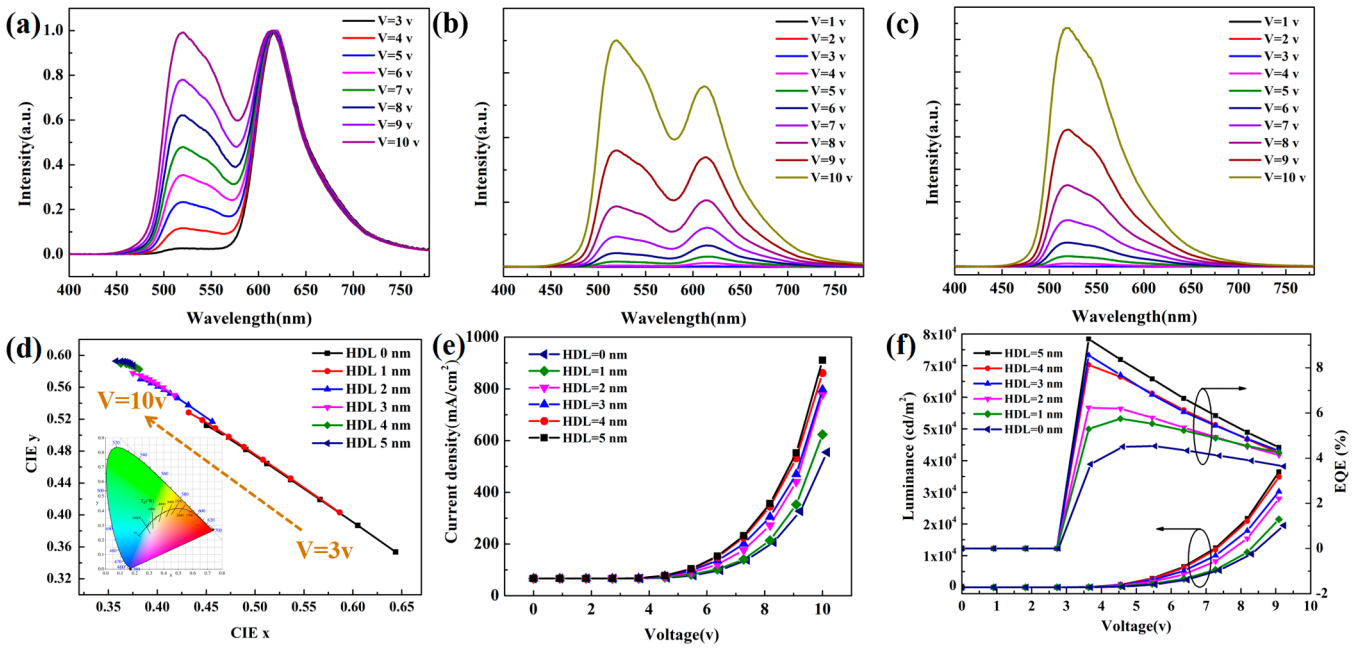

Figure 2. Relationship between the EL spectra of YOLEDs (a) normalized without HDL and with (b) 1 nm HDL and (c) 4 nm HDL. The comparison of (d) CIE color coordinates, (e) *V*−*J* characterization, and (f) *L*−*V*-EQE characterization of OLEDs with the HDL thickness of 0−5 nm.

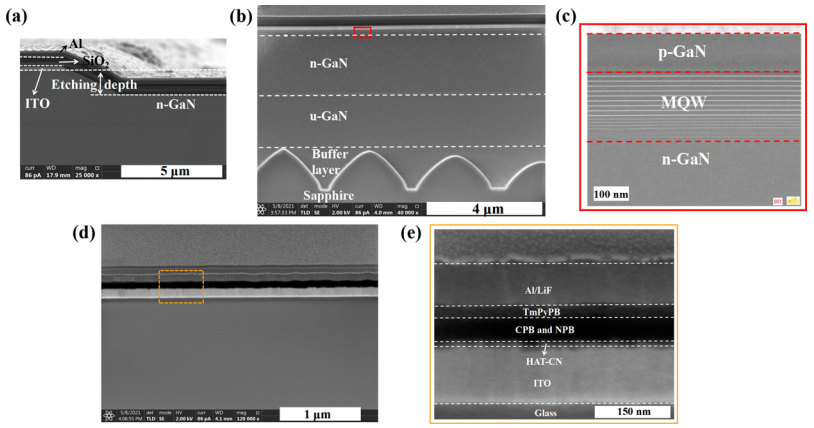

Figure 3. Cross-sectional images of (a) etching mesa and (b) structure of the BLED and the (c) partial enlargement of the red box in (b), and (d) structure of YOLEDs and the (e) partial enlargement of the yellow box in (d).

increase in voltage, the mobility of electrons increased, and the recombination regions of carriers were not only in the red EML but also in the green EML; thus, the green emission grew gradually. The higher the voltage, the stronger the green light intensity and reached the same EL intensity as red emission at 10 V. By incorporating 1 nm HDL between the red EML and the green EML, the intensity of red light increased slowly, while the green light increased more significantly at the same voltage, which was attributed to the hole delay effect of the HDL, leading to the main recombination zone of carriers gradually migrating from the red EML to the green EML. Meanwhile, it was also found that the intensity of green light reached to the equal level of red light at 8 V and exceeded the red light after increasing the voltage, as observed in Figure 2b. Obviously, the thickness of HLD seriously affected the recombination position of carriers. However, the HDL was not as thick as it should be. With the increase in thickness, the ability of the HDL to block holes injected to the red EML was improved. If the HDL was too thick, even at high voltage, the holes would accumulate at the HDL interface and emitted green light only. As vividly illustrated in Figure 2c, when the HDL thickness reached 4 nm, green light instead of yellow light was obtained, as expected. Moreover, the International Commission on Illumination (CIE) color coordinates of the above-mentioned OLED samples were measured and are shown in Figure 2d. As the voltage increased from 3 to 10 V, the CIE values changed from (0.64, 0.35), (0.59, 0.40), (0.46, 0.52), (0.42, 0.55), (0.38, 0.58), and (0.37, 0.59) to (0.45, 0.51), (0.43, 0.53), (0.38, 0.57), (0.38, 0.58), (0.36, 0.59), and (0.36, 0.59), corresponding to the OLEDs without HDL, with 1, 2, 3, 4, and 5 nm HDL, respectively. The color modulation ranges of OLEDs without HDL and with 1 nm HDL were shifted from red to orange-yellow and from orange-red to greenish yellow, respectively, exhibiting a wide color-tunable range. Furthermore, to confirm the function of the HDL on the performance of YOLEDs, the current density−voltage−

https://doi.org/10.1021/acsomega.1c06934
ACS Omega 2022, 7, 5502−5509

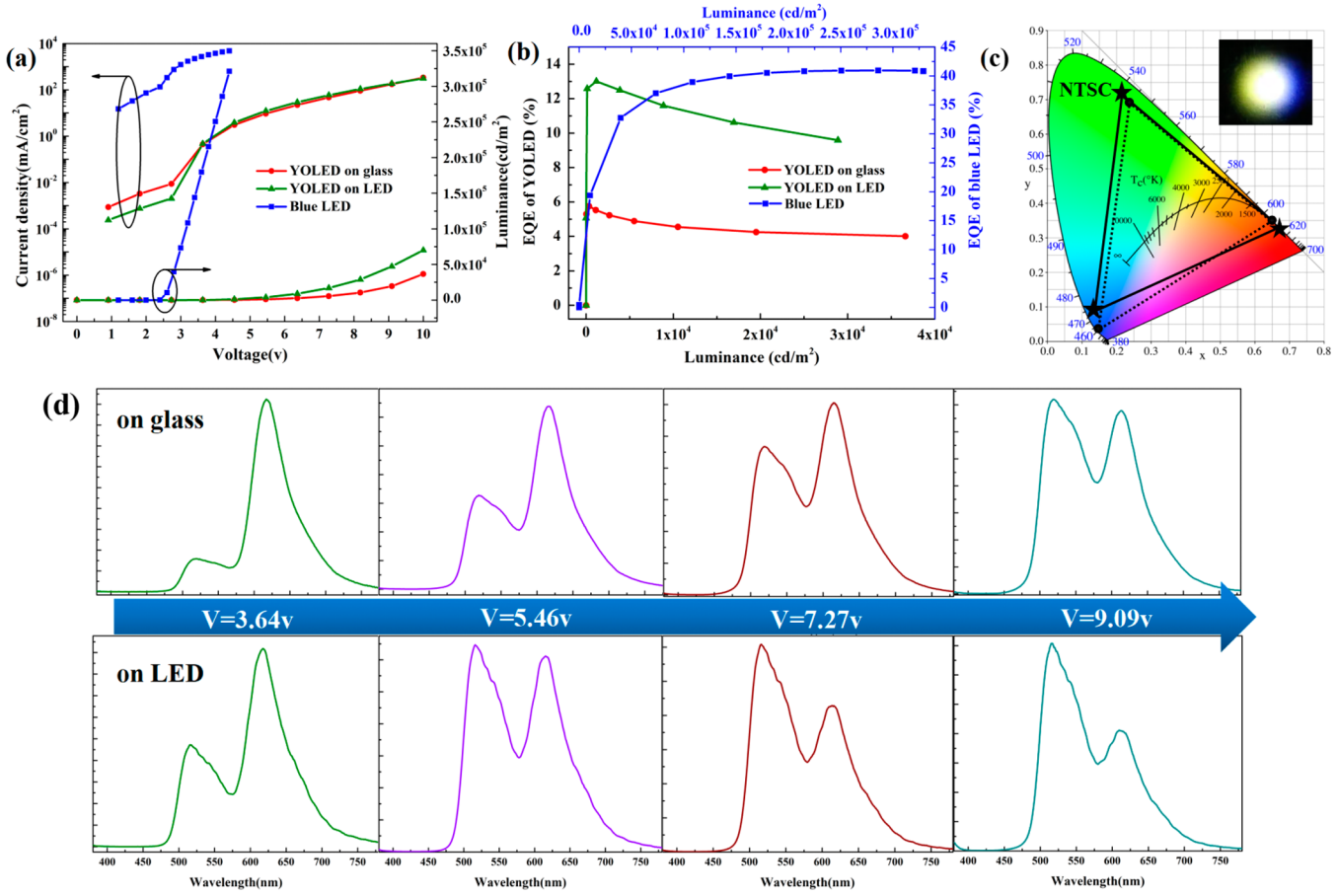

Figure 4. (a) $J-V-L$ and (b) L-EQE characteristics of the BLED and YOLEDs on the LED and the glass substrate. (c) CIE coordinates of the hybrid LED. The inset is an actual emission photo. (d) Normalized EL spectra of YOLEDs on the LED and the glass substrate at different voltages.

luminance ($J-V-L$) and external quantum efficiency (EQE) data were collected and analyzed. As shown in Figure 2e, when the OLED device was working normally, the current density increased with the increase in HDL thickness, but it changed irregularly before being turned on, which may be due to certain unavoidable discrepancies between different batches of samples, or due to experimental errors caused by equipment or measuring. Both the luminance and EQE increased with the increase in HDL thickness after the turned-on voltage, as shown in Figure 2f, indicating that charge balance in the EML has been improved. Taking the electrical performance and color adjustable range into consideration, an OLED with 1 nm HDL was selected as the organic component of the hybrid device.

2.3. Performance of the Color-Tunable Hybrid LED Device. To better evaluate the performance of organic and inorganic hybrid LED devices, the layered structures of both BLEDs and YOLEDs were inspected. As shown in the cross-sectional images of Figure 3, the epitaxial growth of BLEDs was good with unobvious defects, and the thickness of every layer and the etching depth from p-GaN to a portion of n-GaN were consistent with the expectation. The interface between the organic layers of YOLEDs was relatively clear and smooth, as shown in Figure 3d, indicating that the films were uniform. Then, the optical and electrical properties of BLEDs and YOLEDs were measured and analyzed. Their $J-V-L$ and luminance-EQE (L-EQE) characteristics are depicted in Figure 4a,b. The BLEDs and YOLEDs exhibited a low turn-on voltage of 2.4 and 3.5 V and a maximum EQE of 40.94 and 13%, respectively. Moreover, the color gamut of the hybrid LED can reach 95.24% NTSC, and the R_a was as high as 92.4%, as shown in Figure 4c. The inset was the emitting photo of the hybrid LED, which presented a distribution of yellow, white, and blue from left to right. The phenomenon resulted from the diffuser placed on the top of the device to solve the problem that the two lighting elements are apart and emitting light with different colors, for better mix of colors. In the actual lighting applications or large-area lighting panels, the BLED and the YOLED should be assembled as a unit and encapsulated with a lampshade element with reflective coating and diffused film to form a uniform light source. The luminance efficiency of the hybrid LED should be further improved by material or structure optimization, which can also be used to achieve color variation at lower voltages. Interestingly, the YOLED fabricated on the GaN LED was better than that on glass, and both luminance and EQE were significantly improved. This phenomenon may be attributed to the following two reasons. One is the patterned sapphire substrate patterns of the sapphire substrate, which can reduce the total internal reflection and increase the probability of light emission, thus improving the light extraction efficiency. The other is the lower material quality of ITO on GaN LED compared with that on the glass substrate, resulting in reduced mobility of holes, which in turn promoted charge balance, and thus improved the efficiency of the device. Inductively coupled plasma (ICP) etching made n-GaN surface rough, and the thickness of ITO

https://doi.org/10.1021/acsomega.1c06934
ACS Omega 2022, 7, 5502−5509

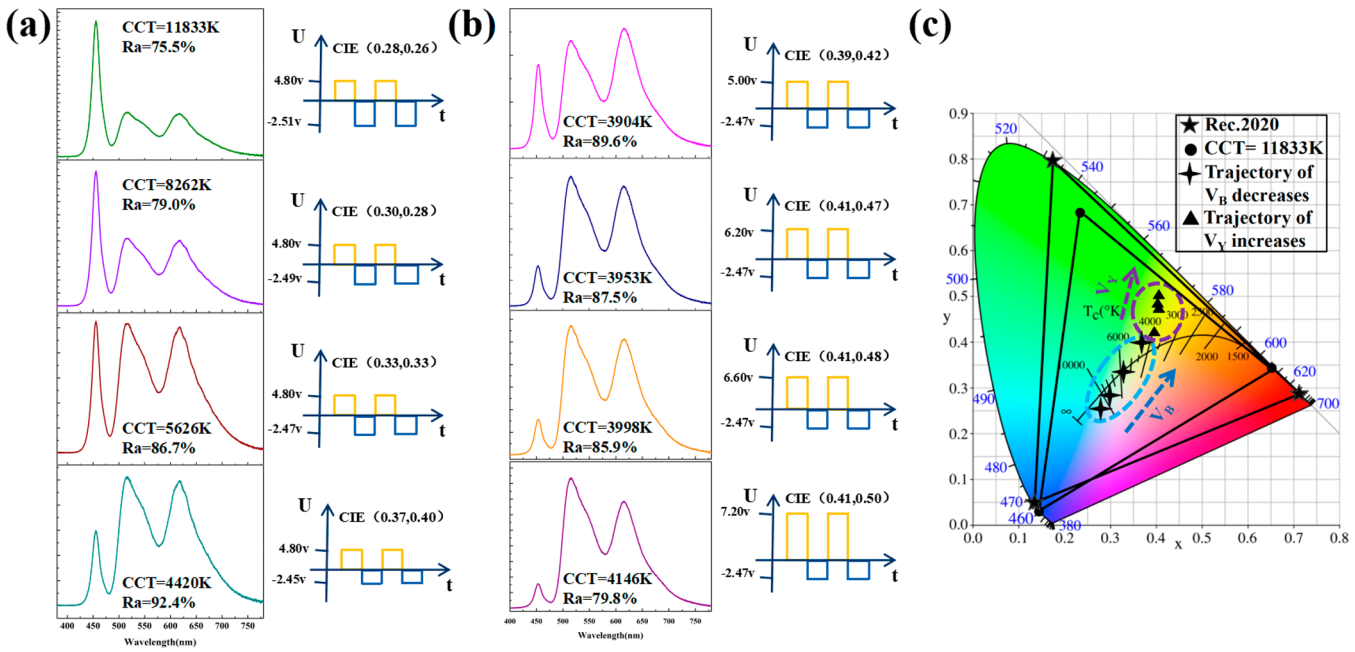

Figure 5. Relationship between the AC-driving voltages and the emitting colors of the color-tunable hybrid LED. (a) V_Y was kept constant, and V_B was adjusted to change the color from cold white to warm white, (b) V_B was kept constant, and V_Y was adjusted to change the color from warm white to yellowish white. (c) CIE coordinates of the hybrid LED varied with the V_Y and the V_B.

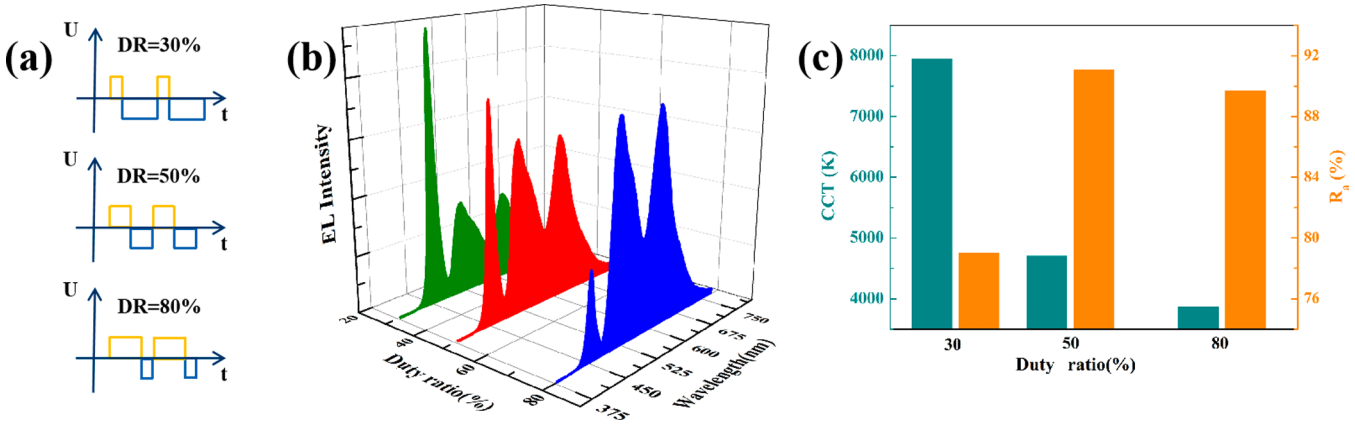

Figure 6. (a) AC-driving signals of different DRs and (b) corresponding EL spectrum and (c) CCT and R_a of the hybrid LED.

on it (150 nm) was smaller than that on the glass substrate (185 nm). These two factors will increase the interface scattering probability and reduce the mobility of carriers in ITO, resulting in the difference in the hole injection velocity into the YOLED; therefore, the main recombination zone of carriers gradually migrate from the red EML to the green EML, resulting in the reduction of current density (only observable at low voltage) in the device on GaN, as shown in Figure 4a. It should be pointed out that at high voltage, the current of the device itself significantly increases by orders of magnitude, and the current density difference caused by the carrier takes a small effect on the total current density, which cannot be detected in the $J-V$ curve, as shown in Figure 4a. To verify this scenario described above, the EL spectra of YOLEDs on the LED and glass substrate at different voltages were measured and are illustrated in Figure 4d. It was clear that the intensity ratio of green light to red light of YOLEDs on the LED was larger than that on the glass substrate at the same voltage. The intensity of green light had already exceeded the red light at 5.46 V, which indicated the mobility of the hole did decrease at the ITO layer on the n-doped GaN substrate.

In order to demonstrate the color-tunable ability of the hybrid LED, AC by positive pulses V_Y and negative pulses V_B was applied, whose amplitude and duration can control the luminance of YOLEDs and BLEDs, respectively. The duty ratio (DR) and frequency of the AC source were set to be 50% and 50 Hz, respectively, so that human eyes perceived a combined emission of BLEDs and YOLEDs. As shown in Figure 5a, the V_Y was set at 4.80 V, and the V_B varied from −2.51 to −2.45 V. With the decrease in V_B, the intensity of the BLED decreased, and the CCT value decreased from 11 833 to 4420 K, while R_a increased from 75.5 to 92.4%. The color of the hybrid LED changed from cold white (0.28, 0.26) to warm white (0.37, 0.40). When the CCT of the hybrid device was 11 833 K, its color gamut was 71.66% Rec.2020, as shown in Figure 5c, suitable for display applications. It was worth noting that the emission intensity of RGB tricolor was nearly equal when the V_B was −2.47 V, and the CIE was (0.33 and 0.33),

https://doi.org/10.1021/acsomega.1c06934
ACS Omega 2022, 7, 5502−5509

which was located very close to the ideal white point of (0.33 and 0.34), with the potential ability of white lighting applications.[46] Based on this, adjusting the amplitude of V_Y can also change the CCT and R_a of the WLED. As depicted in Figure 5b, CCT increased with the increase in V_Y, while R_a decreased gradually. The color of hybrid LED changed from warm white (0.39, 0.42) to yellowish white (0.41, 0.50), which was very suitable for the use of high beam of cars, with the advantages of comfortable light feeling, no glare, and strong penetrability, resulting in the good effect in the weather of rain and fog. Clearly, the emitting color of the hybrid LED was strong dependent on the V_Y and V_B of AC-driving signals. By simply varying the values of V_Y and V_B, the emitting color can be easily controlled, which was intuitively shown in the CIE coordinate chart in Figure 5c, and achieving the function of color temperature adjustable lighting.

Besides the polarity and the amplitude, the DR of the AC-driving signal, which was defined as the proportion of the time occupied by the high level (V_Y) to the whole period time, can also modulate the emitting color of the hybrid LED. Within the same period, different lighting time of BLEDs and YOLEDs will lead to the fluctuation of intensity, resulting in the different performance of the hybrid LED. Herein, 30, 50, and 80% were used to further explore the effect of DR, with the constant voltage and frequency of 50 HZ, as shown in Figure 6a. Then, the collective light, resulting from the photoluminescence of the hybrid LED, was investigated. With the increase in DR, the EL intensity of YOLEDs increased and of the BLEDs decreased, as shown in Figure 6b. Moreover, the CCT and R_a can be altered by tuning the driving time, corresponding to the results drawn in Figure 6c. Thus, by modulating the amplitude and the proportion of V_Y and V_B, a series of white emission with different ratios of yellow and blue emission intensity can be obtained. Specifically, the color coordinates of the white LED can be tuned to trace the blackbody locus for a wide range of CCT (3668−11 833 K); accordingly, color change trend was from cold white to standard white and to yellowish white. The white balance adjustment method is simple and remarkable, which has a great application prospect in lighting. It should be mentioned that in the hybrid device, the luminance of YOLEDs decayed faster than that of LEDs, which should be further improved by adapting better OLED materials and structures.

3. CONCLUSIONS

In summary, a novel and color-tunable hybrid structure of LEDs has been first demonstrated to achieve full white and other colors, with high color gamut and high CRI. Specifically, the hybrid LED consists of inorganic blue GaN LEDs (BLEDs) and YOLEDs, and the color-tunable optical properties could be achieved by adjusting the polarity, amplitude, and DR of AC driving voltages. The intensity of BLEDs can be independently controlled by the negative voltage (V_B), while the intensity and CCT of YOLEDs formed by green and red can be altered by tuning the thickness of the HDL and the negative voltage (V_Y). Therefore, the intensity and proportion of RGB of the hybrid LED are adjustable and bring the difference of emitting color, CCT, and R_a. The hybrid LED device can achieve a wide range of white light from cold white to standard white to warm white (3668−11 833 K), and the highest R_a is up to 92.4%. Compared with the same sized lighting panel, the cost of the hybrid LED device is lower than that of a white OLED and higher than that of a white LED. Phosphors are very cheap, which has obvious cost advantages when combined with LEDs to make the large-area lighting panel. However, the white LED based on phosphors has the disadvantages of color tunability and a narrow color gamut. OLEDs have the characteristics of bright color, high contrast, and color tunability, but their commercial application is greatly hindered by the high cost and the poor lifetime of blue OLEDs. The hybrid device proposed in this paper can solve both issues, which can reduce the cost, achieve a wider color gamut, and achieve color tunability. These results highlight the potential for the novel hybrid device with blue LEDs and OLEDs in smart solid-state lighting, display, and light communication.

4. EXPERIMENTAL SECTION

4.1. Fabrication of the Hybrid LED Device. The hybrid LED consists of BLEDs and YOLEDs connected in parallel but in opposite polarity. The BLED device was prepared by the epitaxial growth technology using metal organic chemical vapor deposition on the *c*-plane sapphire substrates. The BLED structure mainly contained a GaN buffer layer (1.4 μm), a undoped u-GaN (1.8 μm), a Si-doped n-GaN (2.0 μm), InGaN/GaN MQW (200 nm) for emission at 456 nm, and a Mg-doped p-GaN layer (120 nm). Then, soda glass mask with a thickness of 2.3 mm was used as the photomask, and a positive photoresist with a thickness of 2.6 μm was used as the etching mask during the ICP dry etching process to etch the mesa downward until a portion of n-GaN was exposed, with the etching component of Ar, O_2, Cl_2, BCl_3, and N_2 at a rate of 16 Å/s and an etching depth of 1.02 μm. ITO layers with 150 nm was deposited on the top of the BLED structure and on the mesas to form p-type ohmic contacts and the anode of the YOLED structure, respectively, and subsequently patterned using photolithography. Additionally, Ni/Au (60/300 nm) for the n-contact pad and the p-contact was deposited. Afterward, a 500 nm-thick SiO_2 isolation layer was coated onto the sample by electron-beam deposition, covering all the areas except the n-contact pad, the p-contact pad, and the positions reserved for the YOLED structure to prevent short circuit.

After completion of the BLED, the Kurt J. Lesker automatic thermal evaporation system was used to deposit the YOLED layers on the reserved area. HAT-CN, NPB, CBP/Ir(ppy)$_3$ (doping ratio is 10%), TmPyPB (variable), CBP/AT5441 (doping ratio is 16%, and AT5441 is a code given by Guangdong Aglaia Optoelectronic Materials Co., Ltd., whose specific name is bis[2,4-dimethyl-6-[7-(2-methylpropyl)-2-quinolinyl-κN]phenyl-κC](2,4-pentanedionato-κO^2,κO^4)-iridium), TmPyPB, LiF, and Al were deposited on the ITO in sequence at a rate of 0.1, 0.5, 0.5:0.05, 0.5, 0.5:0.08, 0.5, 0.1, and 1 Å/s, respectively, and the thicknesses were 5, 50, 20, 1, 20, 20, 1, and 100 nm, respectively. What is more, the full chip size of the hybrid LED device is 1.5 × 1.5 cm^2, with the thickness of 160 μm, and the effective lighting area of BLED and YOLED is 2 × 1 and 2 × 2 mm^2, respectively.

4.2. Characterization. The evaporation rates and the thicknesses of all the organic layers were in situ-monitored and controlled by the crystal oscillator of the Kurt J. Lesker system. The AC square-wave voltage signals were provided using a function/arbitrary waveform generator (SDG6052X-E, Siglent). A spectrometer (SRC-200, Everfine) was used to measure the EL emission spectra of the devices. The *J*−*V*−*L* characteristics were measured with a semiconductor testing system (Keithley 4200-SCS) and a PR670 spectrometer.

https://doi.org/10.1021/acsomega.1c06934
ACS Omega 2022, 7, 5502−5509

AUTHOR INFORMATION

Corresponding Authors

Xiongtu Zhou − *College of Physics and Information Engineering, Fuzhou University, Fuzhou 350116, PR China; Fujian Science & Technology Innovation Laboratory for Optoelectronic Information of China, Fuzhou 350116, PR China;* orcid.org/0000-0003-3991-3467; Email: xtzhou@fzu.edu.cn

Yongai Zhang − *College of Physics and Information Engineering, Fuzhou University, Fuzhou 350116, PR China; Fujian Science & Technology Innovation Laboratory for Optoelectronic Information of China, Fuzhou 350116, PR China*; Email: yongaizhang@fzu.edu.cn

Qun Yan − *College of Physics and Information Engineering, Fuzhou University, Fuzhou 350116, PR China; Fujian Science & Technology Innovation Laboratory for Optoelectronic Information of China, Fuzhou 350116, PR China*; Email: qunfyan@gmail.com

Authors

Yalian Weng − *College of Physics and Information Engineering, Fuzhou University, Fuzhou 350116, PR China*

Guixiong Chen − *College of Physics and Information Engineering, Fuzhou University, Fuzhou 350116, PR China*

Junyang Nie − *Faculty of Electronic and Information Engineering, Xi'an Jiaotong University, Xi'an 710049, China*

Sihua Que − *College of Physics and Information Engineering, Fuzhou University, Fuzhou 350116, PR China*

Suk-Ho Song − *Department of Electrical and Computer Engineering, Sungkyunkwan University, Suwon 16419, South Korea*

Yongshen Yu − *College of Physics and Information Engineering, Fuzhou University, Fuzhou 350116, PR China*

Fan Zhang − *Fujian Prima Optoelectronics Company Ltd., Fuzhou 350000, PR China*

Hengshan Liu − *Fujian Prima Optoelectronics Company Ltd., Fuzhou 350000, PR China*

Jie Sun − *College of Physics and Information Engineering, Fuzhou University, Fuzhou 350116, PR China; Fujian Science & Technology Innovation Laboratory for Optoelectronic Information of China, Fuzhou 350116, PR China*

Jang-Kun Song − *Department of Electrical and Computer Engineering, Sungkyunkwan University, Suwon 16419, South Korea;* orcid.org/0000-0003-1666-8438

Chaoxing Wu − *College of Physics and Information Engineering, Fuzhou University, Fuzhou 350116, PR China; Fujian Science & Technology Innovation Laboratory for Optoelectronic Information of China, Fuzhou 350116, PR China*

Tailiang Guo − *College of Physics and Information Engineering, Fuzhou University, Fuzhou 350116, PR China; Fujian Science & Technology Innovation Laboratory for Optoelectronic Information of China, Fuzhou 350116, PR China*

Complete contact information is available at: https://pubs.acs.org/10.1021/acsomega.1c06934

Notes

The authors declare no competing financial interest.

ACKNOWLEDGMENTS

This work was financially supported by the National Natural Science Foundation of China (no. 61775038), the National Natural Science Foundation of Fujian Province, China (2019J01221), the Program for New Century Excellent Talents in Fujian Province University, and Fujian Science & Technology Innovation Laboratory for Optoelectronic Information of China (2020ZZ110 and 2021ZZ130).

REFERENCES

(1) Chen, K.-J.; Lai, Y.-C.; Lin, B.-C.; Lin, C.-C.; Chiu, S.-H.; Tu, Z.-Y.; Shih, M.-H.; Yu, P.; Lee, P.-T.; Li, X.; Meng, H.-F.; Chi, G.-C.; Chen, T.-M.; Kuo, H.-C. Efficient hybrid white light-emitting diodes by organic-inorganic materials at different CCT from 3000K to 9000K. *Opt. Express* **2015**, *23*, A204−A210.

(2) Yang, G.; Chen, P.; Gao, S.; Chen, G.; Zhang, R.; Zheng, Y. White-light emission from InGaN/GaN quantum well microrings grown by selective area epitaxy. *Photon. Res.* **2016**, *4*, 17−20.

(3) Verma, A.; Sharma, S. K.; Lin, C.-H.; Manikandan, A.; Kuo, H.-C. Fabrication of highly efficient hybrid device structure based white light emitting diodes. *Opt. Quant. Electron.* **2020**, *52*, 353−363.

(4) Jin, X.; Chen, W.; Li, X.; Guo, H.; Li, Q.; Zhang, Z.; Zhang, T.; Xu, B.; Li, D.; Song, Y. Thick-shell CdZnSe/ZnSe/ZnS quantum dots for bright white light-emitting diodes. *J. Lumin.* **2021**, *229*, 117670−117679.

(5) Sun, W.; Zhou, L.; Zhu, Q.; Wu, R.; Li, Z.; Li, S.; Qin, D. Efficient multi-light-emitting layers warm and pure white phosphorescent organic light-emitting diodes with excellent color stability. *J. Lumin.* **2020**, *228*, 117596−117603.

(6) Peng, D.; Zhang, K.; Chao, V. S.-D.; Mo, W.; Lau, K. M.; Liu, Z. Full-Color Pixelated-Addressable Light Emitting Diode on Transparent Substrate (LEDoTS) Micro-Displays by CoB. *J. Disp. Technol.* **2016**, *12*, 742−746.

(7) Fröbel, M.; Fries, F.; Schwab, T.; Lenk, S.; Leo, K.; Gather, M. C.; Reineke, S. Three-terminal RGB full-color OLED pixels for ultrahigh density displays. *Sci. Rep.* **2018**, *8*, 9684−9690.

(8) Zhang, Y.; Zhuo, P.; Yin, H.; Fan, Y.; Zhang, J.; Liu, X.; Chen, Z. Solid-State Fluorescent Carbon Dots with Aggregation-Induced Yellow Emission for White Light-Emitting Diodes with High Luminous Efficiencies. *ACS Appl. Mater. Interfaces* **2019**, *11*, 24395−24403.

(9) Hu, Z.; Yin, Y.; Ali, M. U.; Peng, W.; Zhang, S.; Li, D.; Zou, T.; Li, Y.; Jiao, S.; Chen, S.-j.; Lee, C.-Y.; Meng, H.; Zhou, H. Inkjet printed uniform quantum dots as color conversion layers for full-color OLED displays. *Nanoscale* **2020**, *12*, 2103−2110.

(10) Li, Y.; Tao, J.; Zhao, Y.; Wang, J.; Lv, J.; Qin, Y.; Liang, J.; Wang, W. 48 x 48 pixelated addressable full-color micro display based on flip-chip micro LEDs. *Appl. Opt.* **2019**, *58*, 8383−8389.

(11) Yang, G. F.; Zhang, Q.; Wang, J.; Lu, Y. N.; Chen, P.; Wu, Z. L.; Gao, S. M.; Chen, G. Q. InGaN/GaN multiple quantum wells on selectively grown GaN microfacets and the applications for phosphor-free white light-emitting diodes. *Phys. Rev.* **2016**, *1*, 101−119.

(12) Zhou, X.; Tian, P.; Sher, C.-W.; Wu, J.; Liu, H.; Liu, R.; Kuo, H.-C. Growth, transfer printing and colour conversion techniques towards full-colour micro-LED display. *Prog. Quant. Electron.* **2020**, *71*, 100263.

(13) Park, K. W.; Kang, T. W.; Kim, D. H.; Park, J. H.; Choi, H. L.; Kim, J. S. Spectral variation of $Y_3Al_5O_12:Ce^{3+}$ nanophosphors and their optical simulation. *J. Lumin.* **2017**, *191*, 40−45.

(14) Zhang, R.; Lin, H.; Yu, Y.; Chen, D.; Xu, J.; Wang, Y. A new-generation color converter for high-power white LED: transparent Ce^{3+}:YAG phosphor-in-glass. *Laser Photon. Rev.* **2014**, *8*, 158−164.

(15) Ye, Y.; Sun, R.; Chen, M.; Tang, H.; Dong, X.; Wang, K.; Wang, Z. Application of an orange−yellow emitting cationic iridium(III) complex in GaN-based warm white light-emitting diodes. *J. Mater. Sci. Mater. Electron.* **2017**, *29*, 1554−1561.

(16) Yu, S.; Tang, Y.; Li, Z.; Chen, K.; Ding, X.; Yu, B. Enhanced optical and thermal performance of white light-emitting diodes with

https://doi.org/10.1021/acsomega.1c06934
ACS Omega 2022, 7, 5502−5509

horizontally layered quantum dots phosphor nanocomposites. *Photon. Res.* **2018**, *6*, 90−98.
(17) Feng, C.; Zheng, X.; Xu, R.; Zhou, Y.; Hu, H.; Guo, T.; Ding, J.; Ying, L.; Li, F. Highly efficient inkjet printed flexible organic light-emitting diodes with hybrid hole injection layer. *Org. Electron.* **2020**, *85*, 105822.
(18) Du, Z.; Zhou, H.; Yu, X.; Han, Y. Controlling the polarity and viscosity of small molecule ink to suppress the contact line receding and coffee ring effect during inkjet printing. *Colloids Surf., A* **2020**, *602*, 125111−125117.
(19) Zheng, X.; Liu, Y.; Zhu, Y.; Ma, F.; Feng, C.; Yu, Y.; Hu, H.; Li, F. Efficient inkjet-printed blue OLED with boosted charge transport using host doping for application in pixelated display. *Opt. Mater.* **2020**, *101*, 109755−109759.
(20) Huang, C.; Zhang, Y.; Zhou, J.; Sun, S.; Luo, W.; He, W.; Wang, J.; Shi, X.; Fung, M. K. Hybrid Tandem White OLED with Long Lifetime and 150 Lm W^{-1} in Luminous Efficacy Based on TADF Blue Emitter Stabilized with Phosphorescent Red Emitter. *Adv. Opt. Mater.* **2020**, *8*, 2000727.
(21) Park, M. J.; Son, Y. H.; Yang, H. I.; Kim, S. K.; Lampande, R.; Kwon, J. H. Optical Design and Optimization of Highly Efficient Sunlight-like Three-Stacked Warm White Organic Light Emitting Diodes. *ACS Photonics* **2017**, *5*, 655−662.
(22) Xiao, P.; Huang, J.; Yu, Y.; Liu, B. Recent Developments in Tandem White Organic Light-Emitting Diodes. *Molecules* **2019**, *24*, 15−42.
(23) Nakamura, K.; Ishikawa, T.; Nishioka, D.; Ushikubo, T.; Kobayashi, N. Color-tunable multilayer organic light emitting diode composed of DNA complex and tris(8-hydroxyquinolinato)-aluminum. *Appl. Phys. Lett.* **2010**, *97*, 193301.
(24) Jou, J.-H.; Wu, M.-H.; Shen, S.-M.; Wang, H.-C.; Chen, S.-Z.; Chen, S.-H.; Lin, C.-R.; Hsieh, Y.-L. Sunlight-style color-temperature tunable organic light-emitting diode. *Appl. Phys. Lett.* **2009**, *95*, 013307.
(25) Ma, Z.; Shi, Z.; Yang, D.; Li, Y.; Zhang, F.; Wang, L.; Chen, X.; Wu, D.; Tian, Y.; Zhang, Y.; Zhang, L.; Li, X.; Shan, C. High Color-Rendering Index and Stable White Light Emitting Diodes by Assembling Two Broadband Emissive Self-Trapped Excitons. *Adv. Mater.* **2020**, *33*, 2001367.
(26) Kuo, Y.-Y.; Huang, C.-C.; Chen, W.-T.; Chang, T.-H.; Lu, H.-C.; Ho, K.-C.; Chao, C.-Y. Widely color-temperature low-luminosity-loss electrochromic-tuned white light-emitting diodes. *Optik* **2020**, *203*, 163994.
(27) Li, J.-S.; Tang, Y.; Li, Z.-T.; Rao, L.-S.; Ding, X.-R.; Yu, B.-H. High efficiency solid−liquid hybrid-state quantum dot light-emitting diodes. *Photon. Res.* **2018**, *6*, 1107−1115.
(28) Feng, T.; Zeng, Q.; Lu, S.; Yan, X.; Liu, J.; Tao, S.; Yang, M.; Yang, B. Color-Tunable Carbon Dots Possessing Solid-State Emission for Full-Color Light-Emitting Diodes Applications. *ACS Photonics* **2017**, *5*, 502−510.
(29) Lien, J.-Y.; Chen, C.-J.; Chiang, R.-K.; Wang, S.-L. High color-rendering flat lamps using quantum-dot color conversion films. *Opt. Express* **2016**, *24*, A1021−A1032.
(30) Liu, Y.; Wei, S.; Wang, G.; Tong, J.; Li, J.; Pan, D. Quantum-Sized SnO_2 Nanoparticles with Upshifted Conduction Band: A Promising Electron Transportation Material for Quantum Dot Light-Emitting Diodes. *Langmuir* **2020**, *36*, 6605−6609.
(31) Chen, S.-W. H.; Huang, Y.-M.; Singh, K. J.; Hsu, Y.-C.; Liou, F.-J.; Song, J.; Choi, J.; Lee, P.-T.; Lin, C.-C.; Chen, Z.; Han, J.; Wu, T.; Kuo, H.-C. Full-color micro-LED display with high color stability using semipolar (20-21) InGaN LEDs and quantum-dot photoresist. *Photon. Res.* **2020**, *8*, 630−636.
(32) Ho, S.-J.; Hsu, H.-C.; Yeh, C.-W.; Chen, H.-S. Inkjet-Printed Salt-Encapsulated Quantum Dot Film for UV-Based RGB Color-Converted Micro-Light Emitting Diode Displays. *ACS Appl. Mater. Interfaces* **2020**, *12*, 33346−33351.
(33) Lin, C.-H.; Verma, A.; Kang, C.-Y.; Pai, Y.-M.; Chen, T.-Y.; Yang, J.-J.; Sher, C.-W.; Yang, Y.-Z.; Lee, P.-T.; Lin, C.-C.; Wu, Y.-C.; Sharma, S. K.; Wu, T.; Chung, S.-R.; Kuo, H.-C. Hybrid-type white LEDs based on inorganic halide perovskite QDs: candidates for wide color gamut display backlights. *Photon. Res.* **2019**, *7*, 579−585.
(34) Cho, J.; Jung, Y. K.; Lee, J.-K.; Jung, H.-S. Surface Coating of Gradient Alloy Quantum Dots with Oxide Layer in White-Light-Emitting Diodes for Display Backlights. *Langmuir* **2017**, *33*, 13040−13050.
(35) Hsu, S.-C.; Ke, L. A.; Lin, H. C.; Chen, T. M.; Lin, H. Y.; Chen, Y. Z.; Chueh, Y. L.; Kuo, H. C.; Lin, C. C. Fabrication of a Highly Stable White Light-Emitting Diode With Multiple-Layer Colloidal Quantum Dots. *IEEE J. Sel. Top. Quant.* **2017**, *23*, 1.
(36) Zhang, H.; Su, Q.; Chen, S. Quantum-dot and organic hybrid tandem light-emitting diodes with multi-functionality of full-color-tunability and white-light-emission. *Nat. Commun.* **2020**, *11*, 2826.
(37) Kim, Y. H.; Koh, S.; Lee, H.; Kang, S.-M.; Lee, D. C.; Bae, B.-S. Photo-Patternable Quantum Dots/Siloxane Composite with Long-Term Stability for Quantum Dot Color Filters. *ACS Appl. Mater. Interfaces* **2020**, *12*, 3961−3968.
(38) Weng, Y.; Chen, G.; Zhou, X.; Yan, Q.; Guo, T.; Zhang, Y. Design and fabrication of bi-functional TiO_2/Al_2O_3 nanolaminates with selected light extraction and reliable moisture vapor barrier performance. *Nanotechnology* **2019**, *30*, 085702.
(39) Lu, Y.; Jia, G.; Wang, G.; Wang, J.; Li, X.; Zhang, C. Novel perovskite quantum dots and hydroxyapatite nanocomposites: Enhanced thermal stability, improved emission intensity, and color-tunable luminescence. *J. Alloys Compd.* **2021**, *861*, 157989.
(40) Xin, J.; Li, Z.; Liu, Y.; Liu, D.; Zhu, F.; Wang, Y.; Yan, D. High-efficiency non-doped deep-blue fluorescent organic light-emitting diodes based on carbazole/phenanthroimidazole derivatives. *J. Mater. Chem. C* **2020**, *8*, 10185−10190.
(41) Su, L.; Cao, F.; Cheng, C.; Tsuboi, T.; Zhu, Y.; Deng, C.; Zheng, X.; Wang, D.; Liu, Z.; Zhang, Q. High Fluorescence Rate of Thermally Activated Delayed Fluorescence Emitters for Efficient and Stable Blue OLEDs. *ACS Appl. Mater. Interfaces* **2020**, *12*, 31706−31715.
(42) Shen, Y.-F.; Zhao, W.-L.; Lu, H.-Y.; Wang, Y.-F.; Zhang, D.-W.; Li, M.; Chen, C.-F. Naphthyridine-based thermally activated delayed fluorescence emitters for highly efficient blue OLEDs. *Dyes Pigm.* **2020**, *178*, 108324.
(43) Yan, Q.; Sun, J.; Nie, J. Y.; Zhou, X. T.; Li, M.; Zhang, Y. A.; Weng, Y. L. A display device having inorganic light-emitting diodes and organic light-emitting diodes connected in parallel but opposite polarity. China Invention Patent CN 202010760395.0 CN 111785714 A, 2020, 1016.
(44) Xing, X.; Zhang, L.; Liu, R.; Li, S.; Qu, B.; Chen, Z.; Sun, W.; Xiao, L.; Gong, Q. A Deep-Blue Emitter with Electron Transporting Property to Improve Charge Balance for Organic Light-Emitting Device. *ACS Appl. Mater. Interfaces* **2012**, *4*, 2877−2880.
(45) Lin, G.; Peng, H.; Chen, L.; Nie, H.; Luo, W.; Li, Y.; Chen, S.; Hu, R.; Qin, A.; Zhao, Z.; Tang, B. Z. Improving Electron Mobility of Tetraphenylethene-Based AIEgens to Fabricate Nondoped Organic Light-Emitting Diodes with Remarkably High Luminance and Efficiency. *ACS Appl. Mater. Interfaces* **2016**, *8*, 16799−16808.
(46) Zhu, Y.; Xu, R.; Zhou, Y.; Xu, Z.; Liu, Y.; Tian, F.; Zheng, X.; Ma, F.; Alsharafi, R.; Hu, H.; Guo, T.; Kim, T. W.; Li, F. Ultrahighly Efficient White Quantum Dot Light-Emitting Diodes Operating at Low Voltage. *Adv. Opt. Mater.* **2020**, *8*, 2001479.

https://doi.org/10.1021/acsomega.1c06934
ACS Omega 2022, 7, 5502−5509